

# Existence of natural mouse IgG mAbs recognising epitopes shared by malondialdehyde acetaldehyde adducts and *Porphyromonas gingivalis*

Innate Immunity  
2021, Vol. 27(2) 158–169  
© The Author(s) 2020  
Article reuse guidelines:  
sagepub.com/journals-permissions  
DOI: 10.1177/11753425920981133  
journals.sagepub.com/home/ini  
SAGE

Mikael Kyrklund<sup>1,2</sup>, Heidi Kaski<sup>1</sup> , Ramin Akhi<sup>1,2</sup>,  
Antti E Nissinen<sup>1,2</sup>, Outi Kummu<sup>1,2</sup>, Ulrich Bergmann<sup>3</sup>,  
Pirkko Pussinen<sup>4</sup> , Sohvi Hörkkö<sup>1,2</sup> and  
Chunguang Wang<sup>1,2,5</sup> 

## Abstract

Natural Abs are produced by B lymphocytes in the absence of external Ag stimulation. They recognise self, altered self and foreign Ags, comprising an important first-line defence against invading pathogens and serving as innate recognition receptors for tissue homeostasis. Natural IgG Abs have been found in newborns and uninfected individuals. Yet, their physiological role remains unclear. Previously, no natural IgG Abs to oxidation-specific epitopes have been reported. Here, we show the cloning and characterisation of mouse IgG mAbs against malondialdehyde acetaldehyde (MAA)-modified low-density lipoprotein. Sequence analysis reveals high homology with germline genes, suggesting that they are natural. Further investigation shows that the MAA-specific natural IgG Abs cross-react with the major periodontal pathogen *Porphyromonas gingivalis* and recognise its principle virulence factors gingipain Kgp and long fimbriae. The study provides evidence that natural IgGs may play an important role in innate immune defence and in regulation of tissue homeostasis by recognising and removing invading pathogens and/or modified self-Ags, thus being involved in the development of periodontitis and atherosclerosis.

## Keywords

Atherosclerosis, malondialdehyde acetaldehyde, natural Ab, periodontitis, *Porphyromonas gingivalis*

Date received: 19 June 2020; revised: 17 November 2020; accepted: 25 November 2020

## Introduction

Inflammation is now widely recognised as a major player in the pathogenesis of atherosclerosis.<sup>1</sup> However, the driving force behind cardiovascular inflammation remains uncertain. Modification of proteins by lipid peroxidation or reactive oxygen species has been shown to associate with the development and progression of atherosclerotic disease.<sup>2,3</sup> Malondialdehyde (MDA) and acetaldehyde (AA), two reactive compounds known to bind covalently to macromolecules, have drawn more attention during recent yr.<sup>3</sup> MDA is generated *in vivo* via peroxidation of polyunsaturated fatty acids, and AA is a major product of ethanol metabolism in the liver or degraded from MDA. Both reactive aldehydes are unstable and can react together in a synergistic manner to form a highly stable hybrid malondialdehyde acetaldehyde

(MAA) adduct.<sup>3,4</sup> MAA adducts possess immunogenic, pro-inflammatory and pro-fibrogenic properties. They

<sup>1</sup>Medical Microbiology and Immunology, Research Unit of Biomedicine, Faculty of Medicine, University of Oulu, Finland

<sup>2</sup>Medical Research Centre and Nordlab Oulu, University Hospital and University of Oulu, Finland

<sup>3</sup>Protein Analysis Core Facility, Biocentre Oulu and Faculty of Biochemistry and Molecular Medicine, University of Oulu, Finland

<sup>4</sup>Oral and Maxillofacial Diseases, University of Helsinki and Helsinki University Hospital, Finland

<sup>5</sup>Minerva Foundation Institute for Medical Research, Biomedicum Helsinki 2U, Finland

## Corresponding author:

Chunguang Wang, Cardiovascular Research Unit, Minerva Foundation Institute for Medical Research, Biomedicum Helsinki 2U, Tukholmankatu 8, Helsinki 00290, Finland.  
Email: chunguang.wang@oulu.fi



are elevated in patients with coronary artery disease and are involved in the initiation and progression of atherosclerosis.<sup>3,5,6</sup> MAA is suggested to be an immunodominant epitope after MDA modification of proteins or lipoproteins, therefore playing a critical role in atherogenesis.<sup>4,5,7</sup>

The oral cavity houses more than 700 bacterial species.<sup>8</sup> The majority of oral microbiome are considered to be commensals that co-occur with low abundance of opportunistic pathobionts. Disruption in harmony of the microbiome leads to dysbiosis, an imbalanced status of the bacterial communities, causing a detrimental shift in the individual components or relative abundances of the microbiome.<sup>9</sup> Dysbiosis of the oral microbiome could initiate conditions such as periodontal diseases that are highly common polymicrobial infections affecting a large portion of the adult population.<sup>10–12</sup> Growing evidence suggests that periodontitis may enhance the risk of several potentially deadly conditions, including cardiovascular diseases.<sup>12,13</sup> Compared to healthy controls, patients with severe periodontitis have increased systemic inflammation, whereas treatment of periodontitis reduces systemic inflammation in patients with or without a history of cardiovascular disease.<sup>12</sup> The major aetiological agents are *Porphyromonas gingivalis* (*Pg*), *Aggregatibacter actinomycetemcomitans* (*Aa*), *Tannerella forsythia* (*Tf*) and *Treponema denticola* (*Td*), the Gram-negative organisms in subgingival plaque biofilm.<sup>14,15</sup> The destruction of the periodontal tissues is mainly due to the host defence against the dysbiotic biofilm.<sup>16</sup> Among the major periodontal pathogens, *Pg* appears to be a keystone pathogen in the development of chronic periodontitis.<sup>12</sup> Colonisation of the host tissues could only happen in the presence of virulence factors such as capsules, fimbriae, LPS, gingipains, outer membrane proteins and outer membrane vesicles.<sup>11</sup> Gingipains, extracellular cysteine proteinases of *Pg*, are one of the major virulence factors responsible for > 85% of the general proteolytic activity generated by this bacterium.<sup>17</sup> There has been no consensus on the best treatment option in the existing literature.<sup>18</sup> The breakdown products from inflammatory tissues can be taken as nutrients by the dysbiotic microbiota. The positive reinforcement between inflammation and dysbiosis make periodontitis a challenging clinical condition. Basic treatments such as scaling, subgingival scaling and root planning cannot abolish the infection, and may also induce complications.<sup>19</sup> Some adjunctive therapies have been studied in recent yr, for example antimicrobial therapy, host modulation therapy, laser therapy and tissue repair and regeneration. However, they are only at the initial phase.<sup>20</sup> There is a need for the development of novel therapeutic approaches with strategies, for example manipulation of microbial

community to restore microbial commensalism from dysbiosis and modulation of the host immune response to limit destructive inflammation.<sup>9,21</sup>

Natural Abs are an essential part of innate immunity. They are produced without external Agic stimulation by B1 B-lymphocytes, marginal zone B cells and other B cell types.<sup>22–25</sup> They are present at birth and include all immunoglobulin classes,<sup>22–25</sup> predominantly IgM and IgA isotypes.<sup>24</sup> The role of natural Abs is to provide a rapid and first-line defence against microbial pathogens and to serve as innate recognition receptors for homeostatic housekeeping functions and removal of altered self-Ags.<sup>26</sup> Among natural Abs, IgM has been extensively studied and shown to bind non-specifically to a broad range of Ags.<sup>22,26–28</sup> For decades, not much attention was paid to the physiological role of natural IgG Abs, as they were thought to be non-reactive. A recent study has shown for the first time that natural IgG recognises a spectrum of bacteria via lectins, such as ficolin and mannose binding protein (MBL), dispelling the general perception that natural IgG Abs lack affinity for pathogens.<sup>23</sup> In this study, we cloned and characterised mouse natural monoclonal IgG Abs recognising MAA adducts. Cross-reactivity of the Abs to a major periodontal pathogen, *Pg*, was also identified.

## Methods

### Bacteria

*Pg* strains ATCC 33277 (a), W50 (b) and OMGS 434 (c) were cultivated on *Brucella* agar plates. *Aa* (ATCC 29523, ATCC 43718, ATCC 33384, IDH 781, IDH 1705, CU1000, C59A, representing six serotypes a, b, c, d, e, f and one non-serotypeable strain x) were grown on fastidious anaerobic agar plates, as described previously.<sup>29,30</sup> *Tf* ATCC 43037 was cultured on NAM plates where 10 µM *N*-acetyl-muramic acid was added to *Brucella* agar. *Escherichia coli* JM109 and *Pseudomonas aeruginosa* ATCC 27853 were grown on LB plates. *Pg*, *Tf* and *P. aeruginosa* were grown under anaerobic conditions. Bacterial cells were suspended in PBS, heat-inactivated at 60°C for 1 h and frozen at –80°C in small aliquots until use. Culture purity was examined by Gram-staining and colony morphology. Protein concentrations were measured by DC™ (detergent compatible) protein assay kit (Bio-Rad, Hercules, CA).

### Cloning of mouse monoclonal IgG

Splenocytes from a low-density lipoprotein (LDL) receptor-deficient mouse (LDLR<sup>-/-</sup>; the Jackson Laboratory, Bar Harbor, ME) were fused with

P3 × 63Ag8.653.1 myeloma cells using a ClonaCell<sup>®</sup>-HY hybridoma cloning kit (Stemcell Technologies UK Ltd., Cambridge, UK). The cells were maintained in growth medium E included in the cloning kit at 37°C with 5% CO<sub>2</sub>. After 10–14 d of growth, hybridoma cell culture media were tested against MAA-LDL and mouse IgG subclass by chemiluminescent immunoassays. Monoclonal hybridoma cell lines were established by sorting a single cell per well on 96-well plates using flow cytometry. The positive clones were propagated and stored in solution containing 85% FBS and 15% DMSO in liquid nitrogen. An IgG isotype control, cIgG, was cloned from a C57BL/6J mouse using the standard polyethylene glycol method.<sup>29</sup>

### Production and purification of mouse IgG mAb

Hybridoma cell culture media were tested for production of IgG against MAA-LDL. Two monoclonal IgG clones (4D5-D5 or HGL+14\_111 and 4F11-E2 or HGL+14\_110) were selected for this study. The hybridoma cells were grown and expanded in growth medium E. After being washed with PBS, the cells were transferred to PFHM-II (protein-free hybridoma medium; Thermo Fisher Scientific, Waltham, MA) and grown for 2 wk. The media were collected and concentrated by Amicon Ultra-15 Centrifugal Filter Units (30 kDa molecular mass cut-off; Millipore, Burlington, MA). Ab purification was carried out with protein G affinity column (Thermo Fisher Scientific), and the purity was checked by SDS-PAGE. The IgG mAbs were isotyped with a Rapid ELISA Mouse mAb Isotyping Kit (Thermo Fisher Scientific) according to the manufacturer's instruction.

### Total RNA isolation, cDNA amplification and sequence analysis

Total RNA from the monoclonal IgG hybridoma cells was isolated with an RNeasy Mini Kit (Qiagen, Valencia, CA). Complementary DNAs (cDNAs) were synthesised with RevertAid Reverse Transcriptase and oligo (dT)18 primers included in the RevertAid First Strand cDNA Synthesis Kit (Thermo Fisher Scientific). The cDNAs were amplified by PCR using the following primers:<sup>31</sup>

IgG heavy chain pair:

forward: MH1 5'-SARGTNMAGCTGSAGSAG TC-3'

reverse: IgG1 5'-ATAGACAGATGGGGGTGTC GTTTTGGC-3'

IgG2A 5'-CTTGACCAGGCATCCTAGAGTCA-3'

IgG2B 5'-AGGGGCCAGTGGATAGACTGA TGG-3'

IgG3 5'-AGGGACCAAGGGATAGACAGATGG-3'  
IgG light chain pair:

forward: 5MK 5'-GAYATTGTGMTSACMCA RWCTMCA-3'

reverse: 3KC 5'-GGATACAGTTGGTGCAGCA TC-3'

The PCR programme for amplification was described previously.<sup>29</sup> The amplified PCR products were purified with a GeneJET PCR purification kit (Thermo Fisher Scientific). The nucleotide sequences were analysed and aligned to the germline genes with the IMGT/V-QUEST sequence alignment tool (www.imgt.org).

### Chemiluminescence immunoassay

Ags were immobilised overnight to Nunc Microfluor2 96-well plates (Thermo Fisher Scientific) in PBS at 4°C. The Ags were MAA-LDL, MDA-LDL, CuOx-LDL (copper-oxidised LDL), Carb-LDL (carbamylation LDL), Native LDL, MAA-BSA (MAA-modified bovine serum albumin), MDA-BSA, PC-BSA (phosphocholine-modified BSA), Carb-BSA, BSA, CWPS (*Streptococcus pneumoniae* cell wall polysaccharide), Rgp44 (gingipain A hemagglutinin domain of *Pg*), *Aa*HSP60 (heat shock protein 60 of *Aa*), *Pg* bacteria mix, *Aa* bacteria mix and FG-PBS (fish gelatin in PBS). Non-specific binding was blocked with 0.5% FG-PBS-0.27 mM EDTA for 1 h at room temperature. The wells were washed using an automated plate washer with PBS-0.27 mM EDTA three times between each step of the immunoassays. The incubation of IgG Ab with different Ags was done at room temperature for 1 h. The binding was detected by alkaline phosphatase labelled with goat anti-mouse IgG (Fc-specific; Sigma-Aldrich, St Louis, MO) followed by LumiPhos 530 substrate (33%; Lumigen, Southfield, MI). The chemiluminescence was determined as relative light units per 100 ms (RLU/100 ms) using a Wallac Victor multilabel reader (PerkinElmer, Waltham, MA). The binding specificity of the IgG Abs to MAA-LDL was examined by a competitive immunoassay. Briefly, the purified IgG Abs were first incubated overnight at 4°C in the presence or absence of different concentrations of competitors (0–100 µg/ml). The Ab and competitor mixtures were centrifuged at 16,000 g for 30 min at 4°C before adding to the microtiter plates with immobilised MAA-LDL (5 µg/ml). The bound Abs were detected in the same way as in the direct binding assay.

### Dot blot and Western blot analysis

Bacterial suspension (20 µg protein/strain/well), MAA-BSA, BSA, MAA-LDL, *Aa*HSP60 and Rgp44 (5 µg/well) in 200 µl of TBS, pH7.6, were loaded onto TBS

pre-wetted nitrocellulose membrane using dot blot apparatus (Bio-Rad). MAA-BSA, MDA-BSA and PC-BSA (10 µg protein/lane) or *Pg* bacterial proteins (25 µg protein/strain/lane) were separated by SDS-PAGE and blotted onto nitrocellulose membranes for Western blotting. All blots were blocked in 5% BSA-TBS, incubated with Ab in 5% BSA-0.05% Tween 20-TBS and washed with 0.05% Tween 20-TBS. The binding to 4D5-D5 and 4F11-E2, 2.5 µg/ml in Dot blot and 0.5 µg/ml in Western blot was visualised by using goat-anti-mouse IgG IRDye800 (0.25 µg/ml; LI-COR Biosciences, Lincoln, NE) as secondary Ab. Isotype control Ab (cIgG, 2.5 µg/ml) was used as a reference. The fluorescent signals were detected with an Odyssey IR imager and Image Studio™ Software (LI-COR Biosciences).

### Protein identification

Cross-reacting proteins were separated by electrophoresis and identified as reported earlier.<sup>32</sup> Briefly, protein bands were excised from SDS gels, treated with dithiothreitol and iocodacetamide to alkylate cysteine side chains and digested with trypsin. Tryptic peptides were subjected to two different approaches of mass spectrometry. First, identification was achieved in off-line mode with a MALDI ToF/ToF mass spectrometry (UltrafleXtreme; Bruker, Billerica, MA) using standard instrument settings and database search parameters.<sup>32</sup> Additionally, the tryptic sample was analysed by LC-MS on a Waters Synapt G2 Q-ToF type mass spectrometer coupled to a nano-Aquity HPLC system with an in-house packed emitter-type column (75 µM × 15 cm) eluted with a 80 min gradient of 0.1% formic acid water/0.1% formic acid in acetonitrile from 3% to 40%. Data were collected in MSE mode and processed with PLGS 2.5 Apex 3D (Waters, Milford, MA). Processed data were used to search the Swissprot database allowing a 4% false-positive rate.

### Flow cytometry analysis of Ab binding to apoptotic cells

Human umbilical vein endothelial cells, EA.hy926, were cultured at 37°C with 5% CO<sub>2</sub> in DMEM (Sigma-Aldrich) supplemented with 10% FBS (Thermo Fisher Scientific), 1 × HAT (hypoxanthine/aminopterin/thymidine) media supplement (Sigma-Aldrich), 100 IU/ml penicillin and 100 µg/ml streptomycin (Sigma-Aldrich). Human Jurkat T cells were grown at 37°C with 5% CO<sub>2</sub> in RPMI-1640 (Sigma-Aldrich) supplemented with 10% FBS (Thermo Fisher Scientific), 100 IU/ml penicillin and 100 µg/ml streptomycin (Sigma-Aldrich), 10 mM Hepes, 2 mM L-glutamine and 1 mM sodium pyruvate. Apoptosis was

induced by starving in FBS-free DMEM for 48 h or by UV-irradiation (20 mJ/cm<sup>2</sup>). The apoptotic cells were identified by DNA staining with SYTOX® AADvanced™ Dead Cell Stain Kit (Life Technologies, Carlsbad, CA). The cells ( $3 \times 10^5$ – $4 \times 10^5$ ) were washed with 0.1% BSA in PBS and centrifuged at 1800 g for 5 min at 4°C. They were incubated with 4D5-D5 or 4F11-E2 Ab (5 µg/ml) with shaking at 4°C for 45 min. Goat anti-mouse IgG (H+L) Alexa Fluor 488 (Invitrogen, Carlsbad, CA) was used as secondary Ab at a concentration of 0.25 µg/ml. The washing was repeated after Ab incubation. Binding of the IgG Abs to apoptotic cells was analysed with FACSCalibur instrument (BD Biosciences, Franklin Lakes, NJ) and FlowJo v10.1 software (FlowJo LLC, Ashland, OR).

## Results

### Cloning of natural mouse monoclonal IgG Abs binding to MAA adducts

To show the biological presence of germline-encoded natural IgG Abs binding to MAA adducts, we isolated and fused splenocytes from a LDLR<sup>-/-</sup> mouse with myeloma cells. Hybridoma growth media were screened against MAA-LDL and IgG subclass by chemiluminescent immunoassay. Monoclonal hybridoma cell lines were established by cell sorting using flow cytometry. Twenty-nine clones binding to MAA-LDL were found after the first cell sorting, five out of them being IgG positive (Figure 1a). These IgG clones (2C8, 2C11, 2E3, 4D5 and 4F11) were sorted one more time to ensure the monoclonal property. After the second cell sorting, seven clones (2C8-F2, 2C11-E8, 2E3-C4, 2E3-E7, 4D5-D5, 4D5-F6 and 4F11-E2) were selected and stored (Figure 1b). Direct binding analysis showed that they all bound to MAA-LDL, and six out of seven clones (all except 4D5-F6) had weak background binding to fish gelatin (Figure 1b).

### IgG clones have high sequence homology with germline genes

To see from which germline gene families these monoclonal IgGs were derived, we analysed sequences of the positive clones by sequencing the PCR products amplified from the cDNAs which were reversely transcribed from the total RNAs isolated from hybridoma cells. The sequences were aligned to germline genes with the IMGT/V-QUEST sequence alignment tool (www.imgt.org). All seven clones originated from the same germline gene family for both heavy and light chains, indicating that they were genetically identical. The V region of heavy chain was derived from IGHV1-



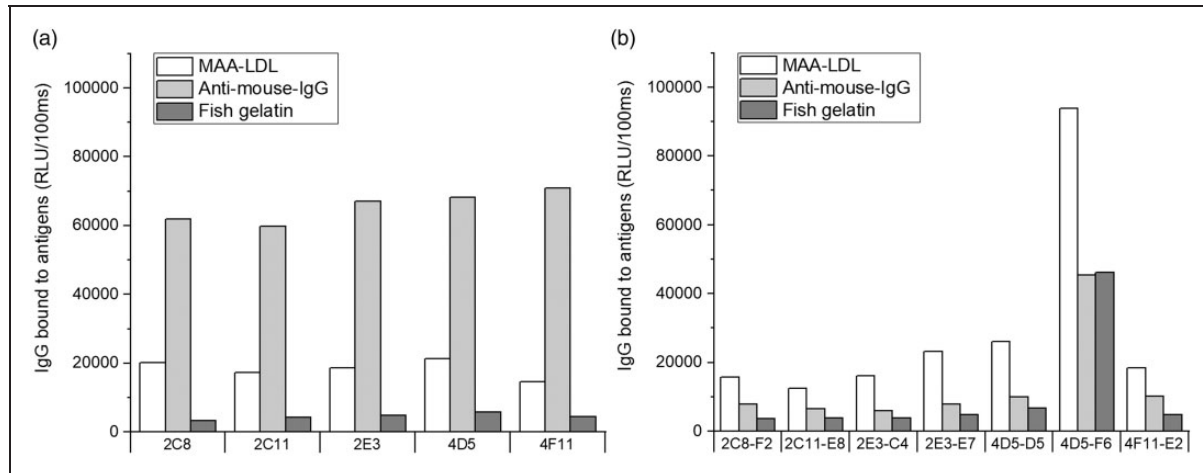


**Figure 1.** Chemiluminescence immunoassays of mouse hybridoma IgG clones bound to malondialdehyde acetaldehyde (MAA) adducts. Direct binding to malondialdehyde acetaldehyde-modified LDL (MAA-LDL), anti-mouse-IgG, and fish gelatin after the first (a) and second (b) cell sorting. RLU: relative light unit.

**Table 1.** Genes encoding  $V_H$  and  $V_L$  from IgG clones against MAA-LDL.

	V Gene	D Gene	J Gene	CDR3
Heavy chain ( $V_H$ )	IGHV1-74*01F 96.53%	IGHD2-3*01F In reading frame 3	IGHJ4*01F 96.30%	CARIYDGYPYAMDYW
Light chain ( $V_L$ )	IGKV12-44*01F 90.76%		IGKJ2*01F 94.74%	CQHYYGIPYTF

74\*01F gene (Table 1). There was one random N nucleotide insertion and one P nucleotide insertion (N1: gcga, P: a) upstream of the D region (V-D joining). A random N nucleotide insertion (N2: tcc) was observed downstream of the D region (D-J junction). The length of heavy chain CDR3 (complementarity-determining region 3) was 13 aa (Table 1). The V region of the light chain originated from the IGKV12-44\*01F gene (Table 1). The identity to germline genes of  $V_H$  and  $V_L$  was about 97% and 91%, respectively, revealing the natural origin of the IgG clones. The monoclonal IgG mAbs were also isotyped. All heavy chains showed positive responses to IgG2b and light chains to kappa ( $\kappa$ ) type.

### Natural IgG mAbs recognise specifically MAA epitopes

To study if the natural IgG mAbs bound to oxidation-specific epitopes, two clones (4D5-D5 and 4F11-E2) having strong MAA-LDL but little background binding were selected for Ab production. After protein G affinity chromatography purification, the purity of the Abs was examined by SDS-PAGE under reducing conditions (Figure 2a). Two major bands of around 50 and 25 kDa, representing heavy and light chains,

respectively, were observed from both clones. The purified natural IgG Abs recognised MAA epitopes on MAA-BSA with no or residual recognition of MDA-BSA and PC-BSA on Western blot (Figure 2b). Isotype control Ab (cIgG) and the secondary Ab alone (2ab, goat anti-mouse IgG IRDye 800) did not bind. In a chemiluminescence immunoassay, both IgG Abs demonstrated strong binding to immobilised MAA-LDL but not to any other Ags tested (Figure 3a and c). The binding specificities of the Abs to oxidised lipid and protein epitopes were determined by competitive liquid-phase immunoassays in the presence or absence of various kinds of competitors (Figure 3b and d). The most specific binding was observed for MAA-LDL, whereas MAA-BSA and MDA-LDL demonstrated partial competition for both IgG Abs. The clone 4D5-D5 seemed to be a more specific and stronger binder to MAA adducts than 4F11-E2 in the chemiluminescence immunoassay.

### IgG mAbs bind to *Pg* strain ATCC33277

To investigate whether the MAA-specific natural IgG Abs have cross-reactivity with pathogenic microbes in periodontitis, the Ab binding to oral bacteria *Aa*, *Pg* and *Tf*, was screened by Dot blot. The binding pattern

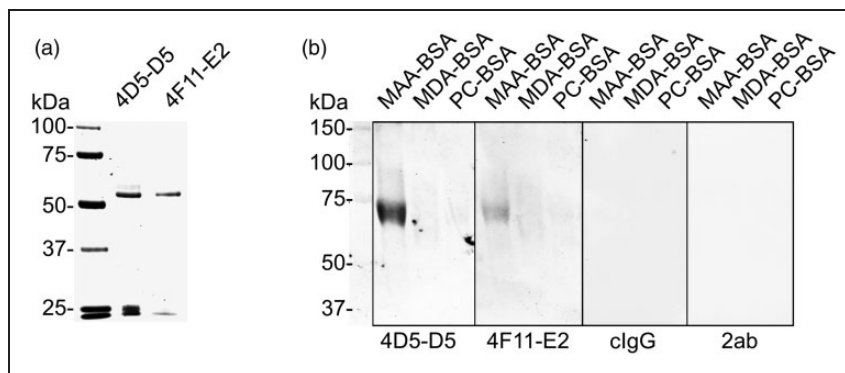


**Figure 2.** SDS-PAGE and Western blot analysis after purification of the natural mouse IgG mAbs. (a) SDS-PAGE after protein G affinity chromatography. Two major bands around 50 and 25 kDa were seen in the 4D5-D5 and 4F11-E2 clones. Precision Plus Protein™ All Blue Prestained Protein Standards (Bio-Rad) was used to indicate molecular mass on the left. (b) Western blot analysis of the natural IgGs. Malondialdehyde acetaldehyde-modified BSA (MAA-BSA), malondialdehyde-modified BSA (MDA-BSA) and phosphocholine-modified BSA (PC-BSA) were loaded into wells (10 µg/lane). A clear band of correct size was visualised from MAA-BSA but not from others after incubation with 4D5-D5 and 4F11-E2 at 1 µg/ml. Goat-anti-mouse-IgG IRDye800 was used as secondary Ab at 0.25 µg/ml. clgG: IgG isotype control; 2ab: secondary Ab alone.

differed between the bacteria tested (Figure 4a). The strongest recognition by both natural IgGs was observed in *Pg(a)* (strain ATCC 33277), whereas *Pg(c)*, *Pg(b)*, *Tf*, *Aa(e)* and *Aa(x)* displayed different extents of binding. No binding to the rest of the *Aa* serotypes (*a*, *b*, *c*, *d*, *f*) or the control bacteria (*E. coli* and *P. aeruginosa*) was found. The secondary Ab alone (2ab) did not show any binding to any of the bacteria tested. MAA-BSA and MAA-LDL were strongly recognised by both natural IgGs, while BSA, *AaHSP60* and *Rgp44* (a lysine specific cysteine proteinase from *Pg*) showed no recognition (Figure 4a). Western blot analysis was performed to verify the IgG binding with *Pg* bacteria. Three protein bands between 50 and 25 kDa were clearly observed in *Pg(a)* (strain ATCC 33277) after incubation with both IgG Abs at a concentration of 0.5 µg/ml (Figure 4b). No recognition was seen in *Pg(b)* (strain W50) and *Pg(c)* (strain OMGS 434). The secondary Ab alone did not recognise any proteins in any of the *Pg* strains. Liquid chromatography–mass spectrometry (LC-MS) analysis was used to identify the recognised proteins further. Lys gingipain (*Kgp*) of *Pg* strain ATCC 33277 was identified from all three protein bands, whereas major fimbrial subunit protein (*FimA* or fimbriillin) type 1 was also found in the middle protein band (Supplemental Table S1).

### *IgG mAbs do not bind to apoptotic cells*

The existence of natural IgG Abs to MAA adduct gave rise to the question of whether they bind to apoptotic cells, behaving similarly to natural IgM Abs. The apoptotic cells were created from human umbilical vein endothelial cells EA.hy926 or from human T lymphocyte Jurkat cells by starving or by UV irradiation.

Flow cytometry analysis revealed that neither of the MAA-specific natural IgG Abs bound to any of the apoptotic cells tested. The results from EA.hy926 cells are shown in Figure 5.

## Discussion

IgG is the predominant Ab class present in mouse and human serum. The knowledge of the existence and physiological role of natural IgGs in immunoregulation and homeostasis is very limited.<sup>23,33</sup> Currently, no natural IgG Abs to oxidation-specific epitopes have been cloned from human or mouse. Here, we report the cloning and characterisation of natural mouse monoclonal IgGs to MAA adducts and their cross-reaction with the key periodontal pathogen *Pg*. Our data suggest that natural IgGs act in innate immune defence and in tissue homeostasis by recognition and removal of invading pathogens and/or altered self-Ags such as oxidised epitopes on LDL.

MAA adduction exists in many tissues and seems to represent a universal example of an inefficient clearance of oxidative stress. MAA is one of the terminal and stable adducts of MDA<sup>7</sup> which functions biologically as a potent immuno-enhancing factor.<sup>34</sup> Both MDA- and MAA-modified LDL particles have been found in atherosclerotic lesions and have been shown to contain immunogenic epitopes recognised by the humoral immune system.<sup>35,36</sup> MAA-modified proteins are strongly associated with early atherosclerosis, vascular inflammation, acute myocardial infarction (AMI) and sudden cardiac death after AMI.<sup>34</sup> MAA adducts are important targets for human natural IgM Abs in neonates and preterm newborns.<sup>4,37</sup> We have previously cloned MAA-specific human Fab Abs and a mouse

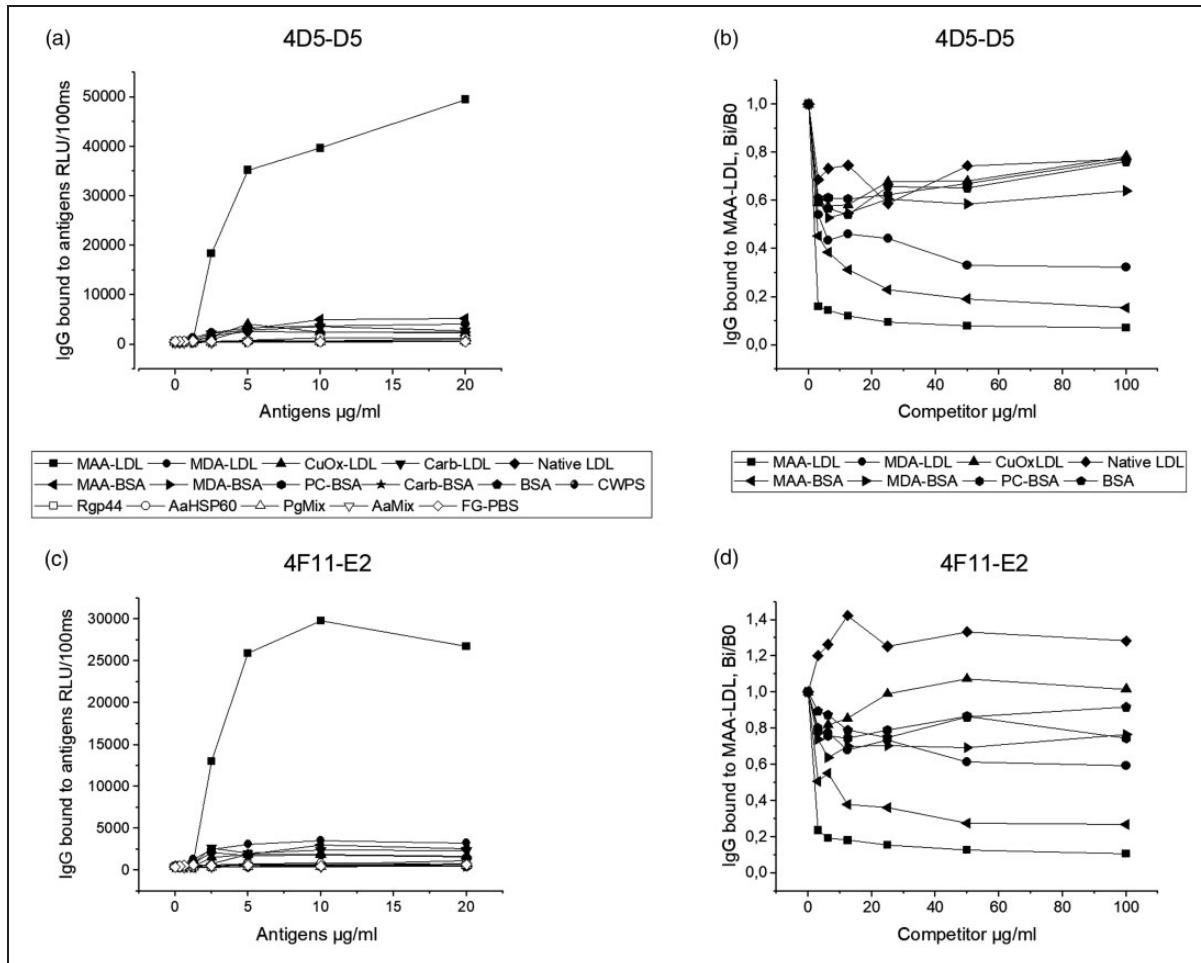


**Figure 3.** Chemiluminescence immunoassays of mouse natural IgG mAbs bound to oxidised epitopes. Direct binding assay for 4D5-D5 (a) and 4F11-E2 (c) to different Ags. The Ags included MAA-modified low-density lipoprotein (MAA-LDL), MDA-modified LDL (MDA-LDL), copper-oxidised LDL (CuOx-LDL), carbamylated LDL (carb-LDL), native LDL, MAA-BSA, MDA-BSA, PC-BSA, carbamylated BSA (carb-BSA), BSA, *S. pneumoniae* cell wall polysaccharide (CWPS), gingipain A hemagglutinin domain of *Pg* (Rgp44), heat shock protein 60 of *Aa* (AaHSP60), *Pg* bacteria mix (three serotypes of *Pg* bacteria), *Aa* bacteria mix (seven serotypes of *Aa* bacteria) and fish gelatin in PBS (FG-PBS). Specific binding to MAA-LDL in competitive liquid-phase chemiluminescence immunoassay for 4D5-D5 (b) and 4F11-E2 (d). The binding is expressed as the binding in the presence of increasing amounts of soluble competitor divided by the binding in the absence of soluble competitors (Bi/B0).

natural IgM mAb cross-reacting with AaHSP60 (heat shock protein 60 of *Aa*).<sup>4,29,30</sup> These natural IgM Abs are suggested to decrease the risk of cardiovascular disease through recognition and clearance of apoptotic cells and immunomodulation of atherogenesis.<sup>1,29,37-39</sup> The existence of IgM Ab to MAA adducts in neonates<sup>4</sup> correlates with the belief that immune activation after oxidative modification of proteins must play some physiological role in protection from deleterious changes to proteins. It has been speculated that low levels of MAA adducts can be rapidly cleared through local scavenger receptors with IgM stimulation. However, an increase in MAA adducts would be induced in chronic and repeated tissue injury, and

thus a shift would be expected in the pathways of scavenger receptor clearance that possibly result in B cell activation and Ab class switching.<sup>34</sup>

IgG Abs are generated through isotype switching and make up the majority of circulating Ab having generally higher affinity than the primary IgM Abs. Human IgGs are divided into four subclasses (IgG1, IgG2, IgG3 and IgG4),<sup>39</sup> and mouse IgGs into IgG1, IgG2a, IgG2b and IgG3, with IgG2c being the equivalent of IgG2a in some mouse strains such as C57BL/6 mice.<sup>40</sup> Both species share > 95% homology in the aa sequences of the Fc regions (constant regions) but show major differences in the aa composition and structure of the hinge region. All subclasses mediate effector

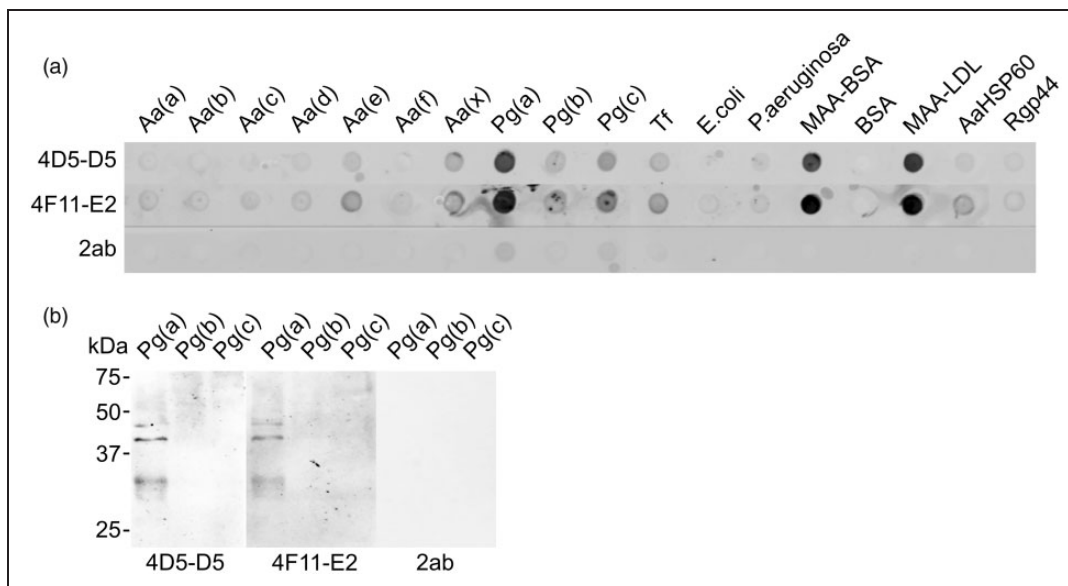


**Figure 4.** Dot blot and Western blot analysis of the monoclonal IgG Abs binding to periodontal bacteria. (a) Dot blot: 20  $\mu$ g whole bacterial protein and 5  $\mu$ g MAA-BSA, BSA, MAA-LDL, AaHSP60 and Rgp44 were loaded per well. 4D5-D5 and 4F11-E2: mouse monoclonal natural IgGs (2.5  $\mu$ g/ml); 2ab: secondary Ab alone (0.25  $\mu$ g/ml); Aa (ATCC 29523, ATCC 43718, ATCC 33384, IDH 781, IDH 1705, CU1000, C59A, representing six serotypes a, b, c, d, e, f and one non-serotypeable strain x); Pg (a: ATCC 33277; b: W50; c: OMGS 434); Tf ATCC 43037. (b) Western blot: 25  $\mu$ g whole bacteria proteins were loaded per lane. Blot was incubated with 4D5-D5, 4F11-E2 and 2ab. Goat-anti-mouse IgG IRDye800 was used as a secondary Ab. Protein molecular masses are indicated on the left.

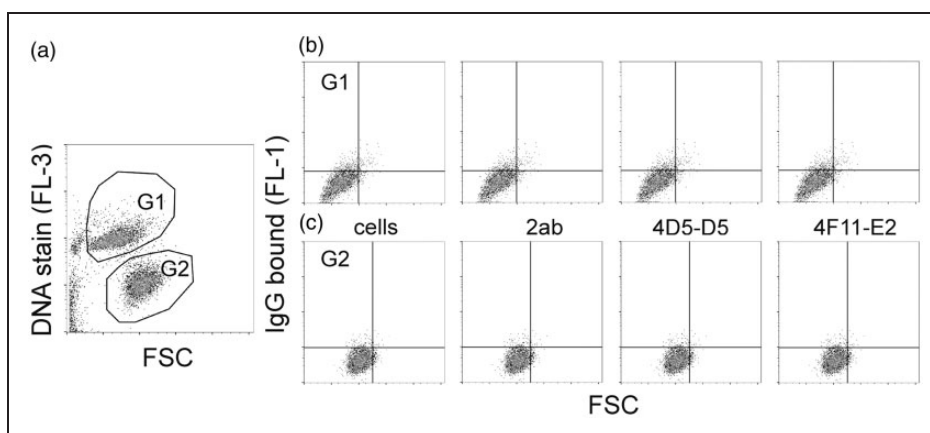


**Figure 5.** Flow cytometry analysis of the natural mouse IgG mAbs binding to apoptotic EA.hy926 cells. (a) Apoptotic cells were created by starving in FBS-free DMEM for 48 h and were populated by DNA staining. G1: apoptotic cells; G2: non-apoptotic cells. (b) Binding of 4D5-D5 and 4F11-E2 to apoptotic cells. (c) Binding of 4D5-D5 and 4F11-E2 to non-apoptotic cells. Cells: the background of cells alone; 2ab: the background of secondary Ab (goat-anti-mouse IgG (H+L), Alexa Fluor 488), 0.25  $\mu$ g/ml; 4D5-D5: 5  $\mu$ g/ml; 4F11-E2: 5  $\mu$ g/ml. Samples were measured in triplicate.

functions, such as Ab-dependent cellular cytotoxicity (ADCC) and complement-dependent cytotoxicity (CDC), slightly differently due to variable specificity and affinity for the different IgG binding partners. IgG2a and IgG2b are the most potent IgG subclasses binding to activating Fc receptors (Fc $\gamma$ RI, Fc $\gamma$ RIII and Fc $\gamma$ RIV) and inhibitory Fc $\gamma$ RIIB with different

affinities.<sup>41,42</sup> In ADCC, the Fc region of an Ab binds to Fc $\gamma$ Rs on the surface of immune effector cells such as NK and macrophages, leading to the phagocytosis or lysis of the targeted cells. In CDC, the Abs kill the targeted cells by triggering the complement cascade at the cell surface. The exact role of natural IgGs in immunoregulation and homeostasis



remains elusive. Recent studies have revealed that natural IgGs recognise and opsonise invading pathogens quickly and effectively, suggesting an essential and immediate protective role in innate immunity.<sup>23</sup> A DNA-delivered IgG mAb has been shown to protect against *P. aeruginosa* in a pneumonia challenge model.<sup>43</sup> Ab-mediated blocking of parasite infection has also been demonstrated by passive transfer of mouse monoclonal IgG Abs recognising the *Plasmodium falciparum* circumsporozoite protein. However, in the study, the IgG subclass was not shown to play any role in influencing *in vivo* efficacy of the Abs.<sup>44</sup> It has been reported that murine IgG1, IgG2a and IgG2b up-regulate Ab responses primarily via Fc $\gamma$ Rs and not via complement. In contrast, IgM and IgG3 act via complement and require the presence of complement receptors 1 and 2 (CR1/2) expressed on both B cells and follicular dendritic cells.<sup>45</sup> IgG2b and IgG3 Abs have also been shown to be particularly important in the early response when T cell help may be limited.<sup>46</sup> We showed in this study that the cloned natural MAA-specific IgG mAbs belonged to the IgG2b subclass, the most potent IgG isotype in mice, and bound to strain ATCC33277 of the keystone pathogen in chronic periodontitis, *Pg*.<sup>12</sup> It can be speculated that the natural IgG2b mAb may act in opsonisation of invading microbes via early Fc $\gamma$ R-mediated effector functions to increase the efficiency of detection and clearance of pathogens and toxins. In addition, the different effector functions, such as those mediated via Fc $\gamma$ R for IgG2b and through complement fixation for IgM,<sup>47</sup> may explain, at least partially, why the natural IgG2b mAb did not bind to apoptotic cells as natural IgMs do. The IgG2b Ab might use ADCC effector mechanism to eliminate invading microbes, whereas natural IgM Ab clears up the apoptotic cells via CDC machinery. This also reveals the importance of matching the isotype with the desired effector function in therapeutic Ab development. Genetic manipulation of the IgG Fc region is occurring to increase or decrease ADCC, complement fixation, glycosylation patterns and neonatal Fc receptor (FcRn) binding to manipulate the effector functions as well as stability and antigenicity.<sup>39,47,48</sup>

The gingipains (RgpA/B and Kgp) of *Pg* have been considered as principle virulence factors that are able to degrade a variety of host proteins and have the potential to dys-regulate host defense.<sup>49</sup> Previous studies have found that they are 'trypsin-like' enzymes secreted by the organism with a variety of different molecular masses and with suggested specificity for cleavage after lysine (Kgp) and arginine residues (RgpA/B).<sup>50</sup> All three proteinases are composed of at least a signal peptide, a propeptide, a catalytic domain, an immunoglobulin-superfamily domain and a C-terminal

domain.<sup>49,51</sup> In addition, Kgp and RgpA have repetitive hemagglutinin-adhesin (HA) domains in the C-terminal regions of the catalytic domains, whereas RgpB lacks the HA domains.<sup>52</sup> Both Kgp and RgpA are subjected to extensive post-translational proteolytic processing and are secreted as non-covalent but very tight complexes of the catalytic and HA domains, which are held together through oligomerisation motifs.<sup>51</sup> Shah et al. found that hemagglutinins and proteinases are closely associated, but still different molecules.<sup>53</sup> It is therefore possible to hypothesise that the close association of the two molecules would be of great benefit to the organism in terms of the sequential binding and degradation of the integral band 3 protein, a transporter responsible for mediating the exchange of chloride (Cl<sup>-</sup>) with bicarbonate (HCO<sub>3</sub><sup>-</sup>) across plasma membranes, causing haemolysis and hemin release.<sup>53</sup> Previously, we have reported that natural IgM to MDA-LDL recognises Rgp44 (aa residues 717–1135 of RgpA),<sup>54</sup> and that immunisation with Rgp44 induces IgM Abs' response to MAA-LDL.<sup>28</sup> It is worthy of notice that in this study, the cloned natural monoclonal MAA-specific IgG mAbs recognised only Kgp but not Rgp44, suggesting that the epitopes on Kgp and Rgp44 may differ from each other, but both share molecular mimicry to MAA adducts.

*Pg* has two distinct fimbria molecules (long and short) on the cell surface that mediate bacterial binding and invasion of host cells. Long fimbriae are classified into six types (I–V and Ib). FimA or fimbrillin type I is the most prevalent among *Pg*-positive healthy adults, whereas type II has significantly greater virulence compared to other types.<sup>55</sup> Long fimbriae enable *Pg* to resist clearance *in vitro* and *in vivo*, promoting its adaptive fitness. Long fimbriae have been shown to be associated with a necessary initial event in the development of atherosclerosis by stimulating endothelial cell activation. Fimbria-mediated invasion has been found to up-regulate the expressions of genes related to inflammation in aortic endothelial cells, leading to accelerated inflammatory responses directly in the aorta. The gene expression of fimA is controlled by the expression levels of the FimA protein itself, as well as by the Rgp and Kgp gingipains. The long fimbriae range from 41 to 49 kDa in size based on their fimbrillin monomer composition. Our findings correspond to the right size of the molecule. Strain W50 with type IV is poorly fimbriated, whereas strain ATCC33277 is an abundantly fimbriated type I strain with significant adhesion to host tissues. We showed that the MAA-specific natural monoclonal IgGs recognised ATCC33277 but not W50, suggesting that the IgGs may be type I specific. Nothing is known about the fimbrillin type on OMGS430 cells. According to our observations, at least it is not type I. Intriguingly, it

has been reported that *Porphyromonas gulae* exhibits virulence and immunological features similar to those of the human periodontal pathogen *Pg*, and thus may have an important role in the development of periodontitis in companion animals. *P. gulae* has been reported to possess FimA that are similar to those of *Pg*. Mice orally inoculated with *P. gulae* elicit a bacterium-specific IgG response and develop alveolar bone resorption similar to that reported for *Pg*.<sup>56</sup>

There is limited information about the role of IgA Abs in periodontitis and in atherosclerosis. Our lab has previously reported that saliva contains IgA and IgG binding to MAA-LDL, which cross-react with *Pg*. The data suggest that secretory IgA to *Pg* may participate in immune reactions involved in LDL oxidation through molecular mimicry, and these Abs may participate in immune reactions involved in atherosclerosis and periodontal disease. However, the levels of salivary IgA and IgG Abs to OxLDL epitopes do not correlate with the levels in plasma.<sup>57</sup> We have also recently shown that salivary IgA to MAA-LDL and oral pathogens are linked to coronary disease.<sup>58</sup> Salivary IgA Ab to MAA-LDL correlates with salivary IgA Ab to oral pathogens including *Pg*. Molecular mimicry between two structurally similar epitopes may have a role in the course of atherosclerosis by activation of cross-reactive immune response, and the results reveal an association between oral humoral response and coronary artery disease. It has also been shown that combined serum IgA and IgG Ab levels to *Aa*, *Pg*, *P. endodontalis*, *P. intermedia*, *Tf*, *Campylobacter rectus* and *Fusobacterium nucleatum* were associated with acute coronary syndrome, while the corresponding subgingival bacterial levels were not.<sup>59</sup> Determining how the innate and adaptive immunity coexist during homeostasis and disease represents a significant direction for future research.

Human periodontitis is affected by the onset of aging. Many factors contribute. However, the age-related remodelling of the immune system, namely immunosenescence, plays a key role.<sup>60,61</sup> The Abs of elderly population seem to be less effective in clearing bacteria. The protective capacity of serum natural IgM generated by B-1a cells decreases considerably with age. Sequence analysis of natural IgM from all B-1a cells demonstrates changes with age by increased N-addition.<sup>62</sup> It has also been observed that not only the percentage of B-1 cells but also their ability to secrete IgM decreased with age.<sup>63</sup> In addition, there have been studies showing that some healthy people do not experience changes in the natural IgM levels, even when they are > 25 yr old, but the natural IgG levels in their circulation rise.<sup>64</sup> There has been a gap in our knowledge about whether aging has an impact on

the protective role of B-1 cell-derived natural Abs and how increasing age affects the existing natural repertoire. Understanding how natural Abs change with age may have potential application in the future.

We showed in the study that the cloned natural monoclonal MAA-specific IgG Abs recognise the most important gingipain Kgp of *Pg* for pathogenesis and the key virulence factor FimA for bacteria colonisation. The cross-reactivity of the MAA-specific natural IgG with oral pathogenic microbes provides evidence that the natural IgGs may play a crucial role in the development of periodontitis and atherosclerosis. The use of natural compounds to attenuate the action of *Pg* has recently gained more attention. With tremendous progress in biomedical studies, exploration of the possible unique mechanism of *Pg* and its virulence determinants will be of help in the development of effective therapies for the tissue destruction in periodontitis. The therapeutic approaches may also be important in controlling chronic *Pg* infections by preventing growth and colonisation of *Pg*. Improved understanding of the interaction between periodontal bacteria and host immune response at the molecular and cellular levels may ultimately have relevance to the overall well-being of the host.

#### Acknowledgements

We gratefully acknowledge Ms Sirpa Rannikko for excellent technical assistance.




#### Declaration of conflicting interests

The author(s) declared no potential conflicts of interest with respect to the research, authorship and/or publication of this article.

#### Funding

The author(s) disclosed receipt of the following financial support for the research, authorship and/or publication of this article: This study was supported by the Research Fund of the Medical Research Center, University of Oulu and Oulu University Hospital, Research Fund of Oulu University Hospital/special state support for research, The Finnish Foundation for Cardiovascular Research and Aarne Koskelo Foundation. The funders had no role in study design, data collection and analysis, decision to publish or preparation of the manuscript.

#### ORCID iDs

Heidi Kaski  <https://orcid.org/0000-0003-2109-9356>  
Pirkko Pussinen  <https://orcid.org/0000-0003-3563-1876>  
Chunguang Wang  <https://orcid.org/0000-0001-5569-321X>

#### Supplemental material

Supplemental material for this article is available online.

## References

1. Tsiantoulas D, Diehl CJ, Witztum JL, et al. B cells and humoral immunity in atherosclerosis. *Circ Res* 2014; 114: 1743–1756.
2. Ho E, Karimi Galougahi K, Liu CC, et al. Biological markers of oxidative stress: applications to cardiovascular research and practice. *Redox Biol* 2013; 1: 483–491.
3. Antoniak DT, Duryee MJ, Mikuls TR, et al. Aldehyde-modified proteins as mediators of early inflammation in atherosclerotic disease. *Free Radic Biol Med* 2015; 89: 409–418.
4. Wang C, Turunen SP, Kummu O, et al. Natural antibodies of newborns recognize oxidative stress-related malondialdehyde acetaldehyde adducts on apoptotic cells and atherosclerotic plaques. *Int Immunol* 2013; 25: 575–587.
5. Gonen A, Hansen LF, Turner WW, et al. Atheroprotective immunization with malondialdehyde-modified LDL is hapten specific and dependent on advanced MDA adducts: implications for development of an atheroprotective vaccine. *J Lipid Res* 2014; 55: 2137–2155.
6. Carson JS, Xiong W, Dale M, et al. Antibodies against malondialdehyde-acetaldehyde adducts can help identify patients with abdominal aortic aneurysm. *J Vasc Surg* 2016; 63: 477–484.
7. Duryee MJ, Klassen LW, Schaffert CS, et al. Malondialdehyde-acetaldehyde adduct is the dominant epitope after MDA modification of proteins in atherosclerosis. *Free Radic Biol Med* 2010; 49: 1480–1486.
8. Aas JA, Paster BJ, Stokes LN, et al. Defining the normal bacterial flora of the oral cavity. *J Clin Microbiol* 2005; 43: 5721–5732.
9. Kleinstein SE, Nelson KE and Freire M. Inflammatory networks linking oral microbiome with systemic health and disease. *J Dent Res* 2020; 99: 1131–1139.
10. Peters BM, Jabra-Rizk MA, O'May GA, et al. Polymicrobial interactions: impact on pathogenesis and human disease. *Clin Microbiol Rev* 2012; 25: 193–213.
11. How KY, Song KP and Chan KG. *Porphyromonas gingivalis*: an overview of periodontopathic pathogen below the gum line. *Front Microbiol* 2016; 7: 53.
12. Hajishengallis G. Periodontitis: from microbial immune subversion to systemic inflammation. *Nat Rev Immunol* 2015; 15: 30–44.
13. Friedewald VE, Kornman KS, Beck JD, et al. The American Journal of Cardiology and Journal of Periodontology Editors' Consensus: periodontitis and atherosclerotic cardiovascular disease. *Am J Cardiol* 2009; 104: 59–68.
14. Socransky SS and Haffajee AD. Periodontal microbial ecology. *Periodontol 2000* 2005; 38: 135–187.
15. Ebersole JL, Dawson D 3rd, Emecen-Huja P, et al. The periodontal war: microbes and immunity. *Periodontol 2000* 2017; 75: 52–115.
16. Kinane DF, Stathopoulou PG and Papananou PN. Periodontal diseases. *Nat Rev Dis Primers* 2017; 3: 17038.
17. Popadiak K, Potempa J, Riesbeck K, et al. Biphasic effect of gingipains from *Porphyromonas gingivalis* on the human complement system. *J Immunol* 2007; 178: 7242–7250.
18. AlAhmari F, Shaikh L and AlDhubaiban D. Photodynamic therapy in the treatment of periodontal diseases: a literature review. *J Int Oral Health* 2020; 12: 102–108.
19. Heitz-Mayfield LJ and Lang NP. Surgical and nonsurgical periodontal therapy. Learned and unlearned concepts. *Periodontol 2000* 2013; 62: 218–231.
20. Li TJ, Wang R, Li QY, et al. Sclerostin regulation: a promising therapy for periodontitis by modulating alveolar bone. *Chin Med J (Engl)* 2020; 133: 1456–1461.
21. Hajishengallis G. Dysbiosis and inflammation in periodontitis: synergism and implications for treatment. *J Oral Microbiol* 2017; 9: 1325198.
22. Grönwall C, Vas J and Silverman GJ. Protective roles of natural IgM Abs. *Front Immunol* 2012; 3: 66.
23. Panda S, Zhang J, Tan NS, et al. Natural IgG antibodies provide innate protection against ficolin-opsonized bacteria. *EMBO J* 2013; 32: 2905–2919.
24. Miller YI, Choi SH, Wiesner P, et al. Oxidation-specific epitopes are danger-associated molecular patterns recognized by pattern recognition receptors of innate immunity. *Circ Res* 2011; 108: 235–248.
25. Pabst O. New concepts in the generation and functions of IgA. *Nat Rev Immunol* 2012; 12: 821–832.
26. Baumgarth N, Tung JW and Herzenberg LA. Inherent specificities in natural antibodies: a key to immune defense against pathogen invasion. *Springer Semin Immunopathol* 2005; 26: 347–362.
27. Hernandez AM and Holodick NE. Editorial: natural antibodies in health and disease. *Front Immunol* 2017; 8: 1795.
28. Kyrklund M, Kummu O, Kankaanpää J, et al. Immunization with gingipain A hemagglutinin domain of *Porphyromonas gingivalis* induces IgM antibodies binding to malondialdehyde-acetaldehyde modified low-density lipoprotein. *PLoS One* 2018; 13: e0191216.
29. Wang C, Kankaanpää J, Kummu O, et al. Characterization of a natural mouse monoclonal antibody recognizing epitopes shared by oxidized low-density lipoprotein and chaperonin 60 of *Aggregatibacter actinomycetemcomitans*. *Immunol Res* 2016; 64: 699–710.
30. Wang C and Hörkö S. Natural monoclonal antibody to oxidized low-density lipoprotein and *Aggregatibacter actinomycetemcomitans*. *Methods Mol Biol* 2017; 1643: 155–167.
31. Wang Z, Raifu M, Howard M, et al. Universal PCR amplification of mouse immunoglobulin gene variable regions: the design of degenerate primers and an assessment of the effect of DNA polymerase 3' to 5' exonuclease activity. *J Immunol Methods* 2000; 233: 167–177.
32. Ullah K, Rosendahl AH, Izzi V, et al. Hypoxia-inducible factor prolyl-4-hydroxylase-1 is a convergent point in the reciprocal negative regulation of NF- $\kappa$ B and p53 signaling pathways. *Sci Rep* 2017; 7: 17220.



33. Huck DM, Okello E, Mirembe G, et al. Role of natural autoantibodies in Ugandans with rheumatic heart disease and HIV. *EBioMedicine* 2016; 5: 161–166.
34. Anderson DR, Duryee MJ, Shurmur SW, et al. Unique antibody responses to malondialdehyde-acetaldehyde (MAA)-protein adducts predict coronary artery disease. *PLoS One* 2014; 9: e107440.
35. Palinski W, Hörkö S, Miller E, et al. Cloning of monoclonal autoantibodies to epitopes of oxidized lipoproteins from apolipoprotein E-deficient mice. Demonstration of epitopes of oxidized low density lipoprotein in human plasma. *J Clin Invest* 1996; 98: 800–814.
36. Hill GE, Miller JA, Baxter BT, et al. Association of malondialdehyde-acetaldehyde (MAA) adducted proteins with atherosclerotic-induced vascular inflammatory injury. *Atherosclerosis* 1998; 141: 107–116.
37. Chou MY, Hartvigsen K, Hansen LF, et al. Oxidation-specific epitopes are important targets of innate immunity. *J Intern Med* 2008; 263: 479–488.
38. Pabst O. New concepts in the generation and functions of IgA. *Nat Rev Immunol* 2012; 12: 821–832.
39. Vidarsson G, Dekkers G and Rispens T. IgG subclasses and allotypes: from structure to effector functions. *Front Immunol* 2014; 5: 520.
40. Zhang Z, Goldschmidt T and Salter H. Possible allelic structure of IgG2a and IgG2c in mice. *Mol Immunol* 2012; 50: 169–171.
41. Nimmerjahn F, Lux A, Albert H, et al. FcγRIV deletion reveals its central role for IgG2a and IgG2b activity *in vivo*. *Proc Natl Acad Sci U S A* 2010; 107: 19396–19401.
42. Beutier H, Gillis CM, Iannascoli B, et al. IgG subclasses determine pathways of anaphylaxis in mice. *J Allergy Clin Immunol* 2017; 139: 269–280.e7.
43. Patel A, DiGiandomenico A, Keller AE, et al. An engineered bispecific DNA-encoded IgG antibody protects against *Pseudomonas aeruginosa* in a pneumonia challenge model. *Nat Commun* 2017; 8: 637.
44. Sack BK, Mikolajczak SA, Fishbaugher M, et al. Humoral protection against mosquito bite-transmitted *Plasmodium falciparum* infection in humanized mice. *NPJ Vaccines* 2017; 2: 27.
45. Sörman A, Zhang L, Ding Z, et al. How antibodies use complement to regulate antibody responses. *Mol Immunol* 2014; 61: 79–88.
46. Collins AM. IgG subclass co-expression brings harmony to the quartet model of murine IgG function. *Immunol Cell Biol* 2016; 94: 949–954.
47. Saxena A and Wu D. Advances in therapeutic Fc engineering – modulation of IgG-associated effector functions and serum half-life. *Front Immunol* 2016; 7: 580.
48. Mahan AE, Jennewein MF, Suscovich T, et al. Antigen-specific antibody glycosylation is regulated via vaccination. *PLoS Pathog* 2016; 12: e1005456.
49. Gorman MA, Seers CA, Michell BJ, et al. Structure of the lysine specific protease Kgp from *Porphyromonas gingivalis*, a target for improved oral health. *Protein Sci* 2015; 24: 162–166.
50. Pike R, McGraw W, Potempa J, et al. Lysine- and arginine-specific proteinases from *Porphyromonas gingivalis*. Isolation, characterization, and evidence for the existence of complexes with hemagglutinins. *J Biol Chem* 1994; 269: 406–411.
51. de Diego I, Veillard F, Sztukowska MN, et al. Structure and mechanism of cysteine peptidase gingipain K (Kgp), a major virulence factor of *Porphyromonas gingivalis* in periodontitis. *J Biol Chem* 2014; 289: 32291–32302.
52. Dashper SG, Mitchell HL, Seers CA, et al. *Porphyromonas gingivalis* uses specific domain rearrangements and allelic exchange to generate diversity in surface virulence factors. *Front Microbiol* 2017; 8: 48.
53. Shah HN, Gharbia SE, Progulske-Fox A, et al. Evidence for independent molecular identity and functional interaction of the haemagglutinin and cysteine proteinase (gingivain) of *Porphyromonas gingivalis*. *J Med Microbiol* 1992; 36: 239–244.
54. Turunen SP, Kumm O, Harila K, et al. Recognition of *Porphyromonas gingivalis* gingipain epitopes by natural IgM binding to malondialdehyde modified low-density lipoprotein. *PLoS One* 2012; 7: e34910.
55. Enersen M, Nakano K and Amano A. *Porphyromonas gingivalis* fimbriae. *J Oral Microbiol* 2013; 5: 10.3402/jom.v5i0.20265.
56. Lenzo JC, O'Brien-Simpson NM, Orth RK, et al. *Porphyromonas gulae* has virulence and immunological characteristics similar to those of the human periodontal pathogen *Porphyromonas gingivalis*. *Infect Immun* 2016; 84: 2575–2585.
57. Akhi R, Wang C, Kyrklund M, et al. Cross-reactive saliva IgA antibodies to oxidized LDL and periodontal pathogens in humans. *J Clin Periodontol* 2017; 44: 682–691.
58. Akhi R, Wang C, Nissinen AE, et al. Salivary IgA to MAA-LDL and oral pathogens are linked to coronary disease. *J Dent Res* 2019; 98: 296–303.
59. Liljeström JM, Paju S, Pietiäinen M, et al. Immunologic burden links periodontitis to acute coronary syndrome. *Atherosclerosis* 2018; 268: 177–184.
60. Fulop T, Le Page A, Fortin C, et al. Cellular signaling in the aging immune system. *Curr Opin Immunol* 2014; 29: 105–111.
61. Poland GA, Ovsyannikova IG, Kennedy RB, et al. A systems biology approach to the effect of aging, immunosenescence and vaccine response. *Curr Opin Immunol* 2014; 29: 62–68.
62. Holodick NE, Vizconde T, Hopkins TJ, et al. Age-related decline in natural IgM function: diversification and selection of the B-1a cell pool with age. *J Immunol* 2016; 196: 4348–4357.
63. Rodriguez-Zhurbenko N, Quach TD, Hopkins TJ, et al. Human B-1 Cells and B-1 cell antibodies change with advancing age. *Front Immunol* 2019; 10: 483.
64. Palma J, Tokarz-Deptula B, Deptula J, et al. Natural antibodies – facts known and unknown. *Cent Eur J Immunol* 2018; 43: 466–475.